

Ab initio simulations of the liquid alloy Au-Cs

Nicolas Charpentier and Jean Cl erouin*

D epartement de Physique Th eorique et Appliqu ee, CEA/DAM  Ile-de-France, Bruy eres Le Ch atel, 91297 Arpajon Cedex, France

(Received 18 July 2008; revised manuscript received 9 September 2008; published 30 September 2008)

We performed quantum molecular-dynamics simulations on the liquid alloy of cesium and gold at a temperature of 900 K in various concentrations. By searching, for each concentration, the zero pressure simulation box, we reproduce the experimental conductivity curve, allowing for a microscopic interpretation of this famous metal to semiconductor transition. The optical properties (absorption and reflectivity) computed at stoichiometry are in agreement with the first observation of transparency of such an alloy in the visible-light range.

DOI: [10.1103/PhysRevB.78.100202](https://doi.org/10.1103/PhysRevB.78.100202)

PACS number(s): 71.15.Pd, 72.15.Cz, 71.30.+h

Since the pioneering experiment of Sommer¹ the sudden transition between metallic behavior and a quasi-insulator of the gold-cesium (Au-Cs) alloy at stoichiometry has stimulated numerous studies (for a review see Ref. 2). In this first experiment, the transition was visualized by the progressive transparency of a gold film in the presence of cesium vapor. Later, a more precise experiment was conducted on the Au-Cs liquid alloy by Hoshino *et al.*³ with a quantitative measurement at normal pressure of the electrical conductivity versus concentration, as shown in Fig. 1. This curve became very popular and is at the origin of many theoretical works. The fascinating question is how a mixture of two very good conductors leads to a poor conductor or a semiconductor. The respective valences of each element and the strong electronegativity of gold immediately suggest a charge trans-

fer according to the octet rule and the formation of dimers. Many theoretical schemes have been proposed, but, to our knowledge, no attempts have been made to use quantum molecular-dynamics (QMD) simulations to study the liquid alloy in contrast with the pure phases. QMD was used to investigate the properties of liquid cesium.⁴⁻⁶ The 0 K isotherm of gold was recently revisited with *ab initio* calculations⁷ and the QMD approach was used to simulate the hot expanded liquid⁸ and aluminum-gold mixtures.⁹ For gold, the importance of relativistic effects was highlighted by Hasegawa and Watabe,¹⁰ which is now taken into account in the generation of the pseudopotentials used in the QMD scheme. Such a microscopic approach can give insights into the electronic structure of the alloys and allows for a direct computation of the structure. Moreover the computed optical-absorption coefficient is a direct response to the first experiment.

We have considered the electronic part of the conductivity, neglecting the ionic conduction [a classical molecular-dynamics (MD) simulation of the ionic part was done by Matsunaga¹¹]. The simulations were performed using projector augmented wave (PAW) pseudopotentials¹² with the electronic structure package VASP developed at the University of Vienna.¹³ Cesium was described by a PAW pseudopotential with 9 active electrons ($5s^25p^66s^1$) and 11 electrons for gold ($5d^{10}6s^1$). This later pseudopotential includes relativistic effects. Both pseudos are using a cutoff of 220 eV and all calculations have been performed with the *high-precision* option. The choice of a good exchange and correlation functional raises a particular question for alloys. Static calculations of the cold curve show that the best choice for cesium is a generalized gradient approximation (GGA) functional, whereas the local-density approximation (LDA) is more adapted for gold. In a density-functional theory (DFT) code the global electronic density cannot satisfy at the same time both functionals (LDA and GGA). We then chose to treat the cesium rich side mixture at the GGA level using the Perdew-Wang parametrization.¹⁴ During the molecular-dynamics simulations the Brillouin zone was sampled at the Γ point. For the electronic conductivity calculations we used more refined k -point sampling: 3^3 in the Monkhorst-Pack scheme.¹⁵ The ionic trajectories were generated for 54 atoms during 1000 time steps of 2 fs after equilibration. Molecular dynamics simulations were performed in the isokinetic ensemble in order to ensure an easier control of the temperatures.

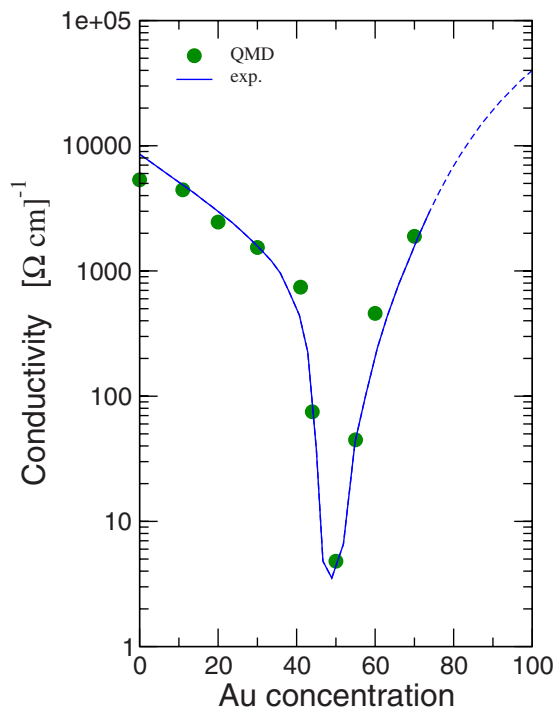


FIG. 1. (Color online) dc conductivity versus concentration of gold atoms. The continuous line is the experiment of Hoshino *et al.* (Ref. 3). Filled circles are QMD computed conductivities obtained after volume optimization. The dashed line corresponds to the solidification of the alloy.

From the knowledge of the Kohn-Sham orbitals ψ_n , energies ϵ_n , and occupations f_n , the conductivity was computed using the Kubo-Greenwood formulation^{17,18} on selected ionic configurations,

$$\sigma(\omega) = \frac{2\pi}{3\omega} \frac{1}{\Omega} \sum_{n,m,\alpha} \sum_{\mathbf{k}} W(\mathbf{k})(f_n - f_m) \times |\langle \psi_n^{\mathbf{k}} | \nabla_{\alpha} | \psi_m^{\mathbf{k}} \rangle|^2 \delta(\epsilon_m^{\mathbf{k}} - \epsilon_n^{\mathbf{k}} - \hbar\omega), \quad (1)$$

where \mathbf{k} and $W(\mathbf{k})$ are the vectors and the weight in the Brillouin zone and ∇_{α} is the velocity operator in each direction ($\alpha=x,y,z$) between two states n and m with occupation numbers f_n and f_m . The dc conductivity is obtained by taking the zero-frequency limit of $\sigma(\omega)$.

We first simulated 54 atoms of cesium at 900 K in a box of 20.1832 Å, leading to a density of 1.50 g/cm³. We checked, by comparing the pair distribution functions, that our structure was in agreement with previous calculations⁴ and with experimental results of Winter *et al.*¹⁹ We got a dc conductivity of 5344 (Ω cm)⁻¹ lower than the experimental results^{20,21} of 7800 (Ω cm)⁻¹ at a density of 1.452 g/cm³ but higher than the result at lower density, 5070 (Ω cm)⁻¹, at a density of 1.332 g/cm³. To build the mixture at different concentrations, a simple substitution of cesium atoms by gold atoms, at constant volume, would lead to inexact results. The Au-Cs mixture, at stoichiometry, is indeed known to exhibit a strong volume contraction of about 48% compared with a linear combination of atomic volumes.²² This volume contraction is particularly strong in this case and follows the curve shown in Fig. 2. Thus, the precise density of the mixture must be determined for each concentration. This has been done by searching the size of the cell corresponding to a vanishing electronic pressure (total pressure minus the ionic kinetic energy). Results of such optimizations are given in Table I and appear not too far from the experimental ones,¹⁶ as shown in Fig. 2. The leading conduc-

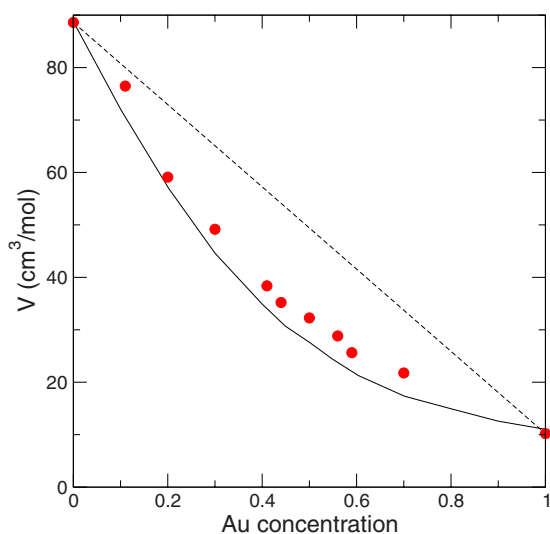


FIG. 2. (Color online) Molar volume as a function of composition. The full line is the experimental data (Ref. 16) and the dashed one the linear combination. Dots are volumes obtained by the optimization of the simulation box.

TABLE I. Volume, densities, and dc conductivities versus concentration in gold atoms. V , ρ , and σ_{dc} are obtained after an optimization of the volume to approach zero electronic pressure.

Gold (% atoms)	N_{Cs}	N_{Au}	V (cm ³ /mol)	ρ (g/cm ³)	σ_{dc} [(Ω cm) ⁻¹]
0	54	0	88.6	1.50	5344
11	48	6	76.5	1.83	4445
20	43	11	59.1	2.47	2455
30	38	16	49.2	3.10	1540
41	32	22	38.4	4.14	743
44	30	24	35.2	4.59	75
50	27	27	32.3	5.11	4.8
56	24	30	28.8	5.84	44.8
59	22	32	25.6	6.66	458
70	16	38	21.8	8.17	1892

tivities, shown in Fig. 1, are in good agreement with the experiments and reproduce the dramatic collapse of conductivity at stoichiometry. It is very interesting to note that, at the minimum of conductivity, a purely ionic conductivity calculation¹¹ with classical effective potentials yields results close to our calculation [a few (Ω cm)⁻¹]. We can consider that the 50% alloy is close to an ionic liquid. However, some discrepancies with the experimental curve of Hoshino *et al.*³ are still observed, which can be traced back to the compromise on the choice of the exchange-correlation functional.

Gaining confidence in the ability of QMD to properly reproduce the underlying physics of this metal-nonmetal transition we now turn to a microscopic interpretation. It is interesting to compare the total pair distribution function at stoichiometry with the experimental results at 910 K as given in Ref. 22. We note in Fig. 3 a general agreement but with slight differences. First, the main peak computed by QMD is higher than the experimental one. Second, the closest approach distance is slightly lower for QMD. In other words, the QMD mixture appears slightly more correlated than the experimental one. We have also compared our QMD simulations with classical MD simulations of Matsunaga¹¹ in Fig. 4. We observe a good agreement for the Au-Cs interactions

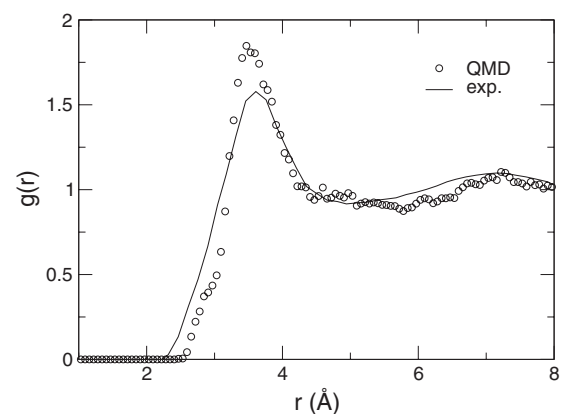


FIG. 3. Total pair distribution function of Au-Cs at stoichiometry. The experimental data are taken at 910 K (Ref. 22).

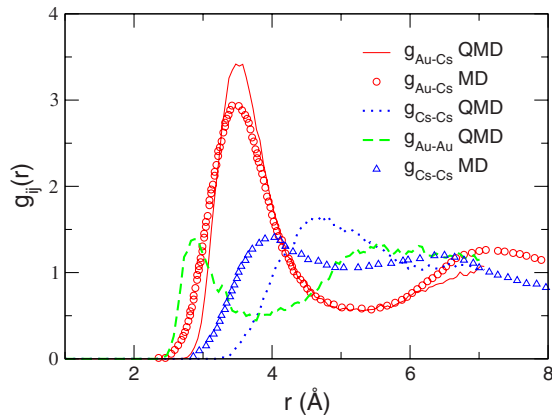


FIG. 4. (Color online) Partial pair distribution functions. Lines are QMD simulations and symbols are taken from classical MD simulations of Matsunaga (Ref. 11).

(line and circles) but the Au-Au and Cs-Cs interactions strongly differ with the MD simulation (triangles). In particular, the QMD pair distribution functions of Au-Au and Cs-Cs are different which is not the case with classical simulations.

Figure 5 shows the total density of states $g(\epsilon)$ and the corresponding total number of electrons integrated over the whole energy range $N(\epsilon) = \int_0^\epsilon f(\epsilon')g(\epsilon')d\epsilon'$, where $f(\epsilon)$ is the usual Fermi-Dirac distribution function. The filled surface corresponds to occupied states $f(\epsilon)g(\epsilon)$. For pure cesium with 54 atoms (top) we recognize the fully occupied $5s$ orbital ($2 \times 54 = 108$ electrons), the fully occupied $5p$ orbital ($6 \times 54 = 324$ electrons), and the singly occupied $6s$ orbital ($1 \times 54 = 54$ electrons). When about 10% of gold is substituted (48 cesium and 6 gold) the $5s$, $5p$, and $6s$ remain almost unchanged and a new peak appears corresponding to $5d$ and $6s$ for gold. A precise counting of electrons shows, however, that six $6s$ cesium electrons have already moved in the

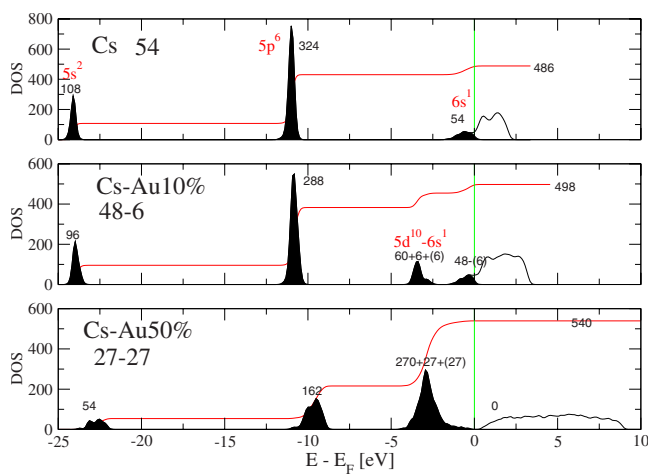


FIG. 5. (Color online) Density of states for pure cesium (top), 10% Au-Cs mixture (middle), and 50% Au-Cs mixture (bottom). The filled surface represents the occupied states. The continuous red (gray) horizontal line gives the total number of electrons and the vertical line the Fermi level. Total numbers of electrons are indicated for each atomic level.

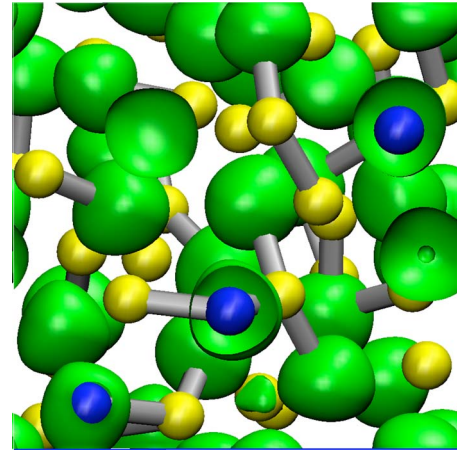


FIG. 6. (Color online) ELF functional (green). Cs ions are represented by blue (dark gray) spheres and gold ions by yellow (light gray) spheres. Bonds correspond to interatomic length of less than 3.5 \AA .

gold band (numbers are indicated between parentheses). The picture changes dramatically at stoichiometry (27 cesium and 27 gold) (bottom). The well identified $6s$ contribution of cesium was now empty and merged in a massive contribution at -3 eV containing hybridized $5p$ and $6s$ states. At the same time we observe the opening of a well defined gap at the Fermi level. A Bader²³ decomposition of charge density leads to a charge transfer from cesium to gold of 0.8 electrons averaged over all atoms. A conventional three-dimensional (3D) representation of some level of the electronic density does not give much information since the electronic density maximum value is always centered on gold ions. More instructive is the electron localization function (ELF) functional, which defines the topology of the system as introduced by Becke and Edgecombe.²⁴ This function is represented with a level of 0.5 in Fig. 6 for the 50% Au-Cs

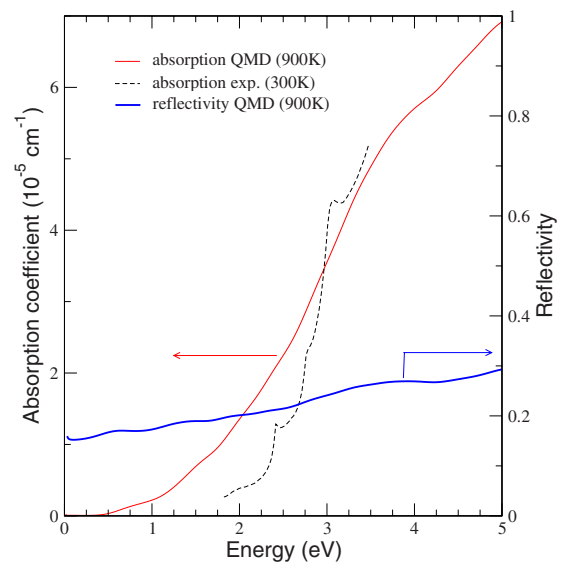


FIG. 7. (Color online) Absorption coefficient of the liquid at 900 K (left scale) compared with the experimental result of Spicer *et al.* (Ref. 27) in the solid phase at 300 K. Right scale: reflectivity.

mixture using the visual molecular-dynamics (VMD) package.²⁵ Cesium ions are represented by blue (dark gray) spheres and gold by yellow (light gray) ones. The chosen isovalue shows a strongly localized functional on cesium atoms, which corresponds to the filled ($5s-5p$) orbital. There are no electrons shared by the two species. Bonds correspond to an interatomic length of less than 3.5 Å, which is in close agreement with the calculation of the Au-Cs dimer. Many examples of such systems (a large green blob attached to gold ions by a bond) can be identified in Fig. 6. We conclude that the representation of the ELF functional characterizes ionic bonding.

To return to the first experimental evidence, we have computed the reflectivity and the absorption coefficient at stoichiometry for liquid Au-Cs at 900 K (for a detailed description of the computation of optical properties from QMD see Ref. 26). The result is compared in Fig. 7 with the experimental result obtained by Spicer *et al.*²⁷ at lower temperature and on the solid. The overall agreement is good although we do not observe the excitonic peaks at 2.6, 3, and 3.3 eV, characteristic of a semiconductor. The difference with the experimental result can be traced back not only to the difference in the temperatures but also to the DFT which is not able to handle properly the insulator gaps.²⁸ The low level of

reflectivity in the range of 2–3 eV ($\approx 20\%$), combined with a rather low value of the absorption in the same range, explains the observation made by Sommer¹ of an *extremely transparent AuCs layer*.²⁹

In summary, we have performed a series of quantum molecular-dynamics simulations on liquid Au-Cs alloy with varied concentrations of gold and at a temperature of 900 K. By computing the electrical conductivity, we have successfully reproduced the well-known sharp minimum of more than 3 orders of magnitude. This minimum is linked to a metal to semiconductor transition and to the opening of a gap. We have also reproduced the observed contraction of the volumes of about 48% which is known to be one of the largest for such alloys. A detailed study of the density of states clearly shows the electron transfer between cesium and gold. The structure of the liquid alloy is obtained and the leading optical properties are compared with experiments.

We wish to thank Pr. Hensel for having drawn our attention to the conductivity of liquid alloys and J. B. Maillet for his help on Bader decomposition. B. Siberchicot, S. Mazevet, and A. Decoster are acknowledged for discussions and careful reading, as well as M. Delaveau for her technical support.

*jean.clerouin@cea.fr

¹A. H. Sommer, *Nature (London)* **152**, 215 (1943).

²J. E. Enderby and A. E. Barnes, *Rep. Prog. Phys.* **53**, 85 (1990).

³H. Hoshino, R. W. Smutzler, and F. Hensel, *Phys. Lett.* **51A**, 7 (1975).

⁴Benedito Jose Costa Cabral and J. L. Martins, *Phys. Rev. B* **51**, 872 (1995).

⁵S. Falconi and G. J. Ackland, *Phys. Rev. B* **73**, 184204 (2006).

⁶B. R. Gelchinski, A. A. Mirzoev, Y. S. Mitrohin, and E. V. Dyulidina, *J. Non-Cryst. Solids* **353**, 3480 (2007).

⁷A. Dewaele, M. Torrent, P. Loubeyre, and M. Mezouar, *Phys. Rev. B* **78**, 104102 (2008).

⁸P. Renaudin, V. Recoules, P. Noiret, and J. Clérouin, *Phys. Rev. E* **73**, 056403 (2006).

⁹J. Clérouin, V. Recoules, S. Mazevet, P. Noiret, and P. Renaudin, *Phys. Rev. B* **76**, 064204 (2007).

¹⁰A. Hasegawa and M. Watabe, *J. Phys. F: Met. Phys.* **7**, 75 (1977).

¹¹S. Matsunaga, *J. Non-Cryst. Solids* **312-314**, 409 (2002).

¹²G. Kresse and D. Joubert, *Phys. Rev. B* **59**, 1758 (1999).

¹³G. Kresse and J. Hafner, *Phys. Rev. B* **47**, 558 (1993).

¹⁴J. P. Perdew and Y. Wang, *Phys. Rev. B* **33**, 8800 (1986).

¹⁵H. J. Monkhorst and J. D. Pack, *Phys. Rev. B* **13**, 5188 (1976).

¹⁶A. Kempf and R. W. Schmützler, *Ber. Bunsenges. Phys. Chem.* **84**, 5 (1980).

¹⁷R. Kubo, *J. Phys. Soc. Jpn.* **12**, 570 (1957).

¹⁸D. A. Greenwood, *Proc. Phys. Soc. Jpn.* **71**, 585 (1958).

¹⁹R. Winter, W.-C. Pilgrim, and F. Hensel, *J. Non-Cryst. Solids* **156-158**, 9 (1993).

²⁰F. Noll, W.-C. Pilgrim, and R. Winter, *Z. Phys. Chem., Neue Folge* **156**, 303 (1988).

²¹R. Redmer, H. Reinholz, G. Röpke, R. Winter, F. Noll, and F. Hensel, *J. Phys.: Condens. Matter* **4**, 1659 (1992).

²²F. Hensel, *Z. Phys. Chem., Neue Folge* **154**, 201 (1987).

²³R. Bader, *Atoms in Molecules: A Quantum Theory* (Oxford University Press, New York, 1990).

²⁴A. D. Becke and K. E. Edgecombe, *J. Chem. Phys.* **92**, 5397 (1990).

²⁵W. Humphrey, A. Dalke, and K. Schulten, *J. Mol. Graphics* **14**, 33 (1996).

²⁶S. Mazevet, M. P. Desjarlais, L. A. Collins, J. D. Kress, and N. H. Magee, *Phys. Rev. E* **71**, 016409 (2005).

²⁷W. E. Spicer, A. H. Sommer, and J. G. White, *Phys. Rev.* **115**, 57 (1959).

²⁸Y. Laudernet, J. Clérouin, and S. Mazevet, *Phys. Rev. B* **70**, 165108 (2004).

²⁹The observed transparency of experimental films of a few hundred angstrom thickness is compatible with an absorption coefficient of $(2-3) \times 10^5 \text{ cm}^{-1}$.